

# Comfetch: Federated Learning of Large Networks on Memory-Constrained Clients via Sketching

Tahseen Rabbani,<sup>1</sup> Brandon Feng,<sup>1</sup> Yifan Yang,<sup>1</sup> Arjun Rajkumar,<sup>1</sup> Amitabh Varshney,<sup>1</sup> Furong Huang<sup>1</sup>

<sup>1</sup> University of Maryland, College Park  
{trabbani, yfeng97, yang7832, rajkumar, varshney, furongh}@umd.edu

## Abstract

A popular application of federated learning is using many clients to train a deep neural network, the parameters of which are maintained on a central server. While recent efforts have focused on reducing communication complexity, existing algorithms assume that each participating client is able to download the current and full set of parameters, which may not be a practical assumption depending on the memory constraints of clients such as mobile devices. In this work, we propose a novel algorithm `ComFetch`, which allows clients to train large networks using compressed versions of the global architecture via Count Sketch, thereby reducing communication and local memory costs. We provide a theoretical convergence guarantee and experimentally demonstrate that it is possible to learn large networks, such as a deep convolutional network and an LSTM, through federated agents training on their sketched counterparts. The resulting global models exhibit competitive test accuracy when compared against the state-of-the-art `FetchSGD` and the classical `FedAvg`, both of which require clients to download the full architecture.

## 1 Introduction

Federated learning is an emerging setting of machine learning which has gained considerable interest within the last few years (Kairouz et al. 2019). In centralized federated learning a set of clients, such as mobile devices, collaboratively solve a machine learning problem under the coordination of a central server. This paradigm has found use in a wide breadth of tasks such as speech prediction, document classification, autonomous vehicle networking, and drone-assisted disaster response (Brisimi et al. 2018; Jiang et al. 2019; Pokhrel and Choi 2020; Pokhrel 2020).

**Memory-Constrained Clients** In federated learning of a neural network, clients assist the server with training a centrally-hosted global model using their own local data. At every iteration, clients download the current and full architecture followed by a local gradient computation which is subsequently communicated to the central server. However, memory-constrained clients such as mobile devices would face difficulty downloading larger models such as deep convolutional networks (Krizhevsky 2009; He et al. 2016), transformers (Vaswani et al. 2017), and LSTMs (Hochreiter and Schmidhuber 1997; Sherstinsky 2020), which can

contain up to several billion parameters. Consequently, deep learning towards mobile applications faces a resource challenge as state-of-the-art models continue to grow without bound (Wang et al. 2018; Deng 2019).

There has been an abundance of progress towards communication-efficiency of the gradient transmissions (Konečný et al. 2016; Haddadpour et al. 2021; Ivkin et al. 2019; Rothchild et al. 2020). For example, the state-of-the-art `FetchSGD` (Rothchild et al. 2020) uses the Count Sketch data structure (Charikar, Chen, and Farach-Colton 2002) to compress each client’s local gradient, greatly reducing communication bandwidth costs. However, to the best of our knowledge, no work has addressed the cost of hosting large models in local client memory.

In this paper, we propose a novel federated learning algorithm, `ComFetch`, which allows memory-constrained clients to train a large global model by computing local gradients with respect to a smaller model. `ComFetch` compresses the weights of the *entire* global architecture via Count Sketches, which are data structures commonly used for lower-dimensional projections with desirable  $\ell_2$ -recovery guarantees (Charikar, Chen, and Farach-Colton 2002). The central server transmits these reduced weights along with the corresponding unsketching maps to the client. The client then computes the gradient with respect to the sketched weights and uploads them to the server. Since these sketched models are cheaper to transmit, we not only improve local memory costs, but also improve communication efficiency *for free*.

`ComFetch` does not come without challenges. While other gradient compression methods are solely concerned with controlling the error associated with compressing (and imperfectly decompressing) outgoing gradients (Spring et al. 2019; Ivkin et al. 2019; Rothchild et al. 2020; Haddadpour et al. 2021), we must contend with gradient approximation error resulting from inexact weight approximations. To control such error, we use an error feedback scheme (Karimireddy et al. 2019) which is shared with other federated learning algorithms such as `Sketched SGD` (Ivkin et al. 2019) and `FetchSGD` (Rothchild et al. 2020).

**Our contributions** (1) We provide a federated learning algorithm called `ComFetch` which allows memory-constrained clients to train a large network. In compar-

ison to federated learning with full architecture downloads, `ComFetch` greatly reduces memory overhead and communication costs. (2) We experimentally demonstrate that `ComFetch` training converges to global models with test accuracies that are competitive against the state-of-the-art `FetchSGD` and significantly better than the baseline `FedAvg`. Furthermore, we observe that using a single Count Sketch (as opposed to the median of several independent sketches), sufficiently results in performance-preserving models up to 4x compression. (3) We propose a communication-efficient backpropagation scheme for taking the gradient with respect to the sketched weights. (4) We provide a probabilistic convergence guarantee for multi-sketch `ComFetch`.

## 2 Preliminaries and Problem Setup

In this section, we outline the objectives and assumptions of our federated learning setting. `ComFetch` is compatible (but not exclusively) with fully-connected networks and convolutional networks, so we also review notations common to these types of models.

**Federated Learning Setup.** We have  $C$  clients and a central server. Let  $\mathcal{D} = \mathcal{X} \times \mathcal{Y}$  be a global data set, where  $\mathcal{X}$  and  $\mathcal{Y}$  are the feature space and label space, respectively. Let  $\{\mathcal{D}_i\}_{i=1}^C$  be the (possibly non-iid) collection of our local client data distributions over  $\mathcal{D}$ . For example,  $\mathcal{D}$  could be the set of all birds labelled by species, and the  $\mathcal{D}_i$  could be regional subsets. Given a loss function  $\mathcal{L} : \mathcal{W} \times \mathcal{D} \rightarrow \mathbb{R}$ , where  $\mathcal{W}$  is a hypothesis class parameterized by matrices, our goal is to minimize the aggregated risk function,

$$f(W) = \frac{1}{\sum_{i=1}^C N_i} \sum_{i=1}^C N_i \mathbb{E}_{z \sim \mathcal{D}_i} \mathcal{L}(W, z), \quad (1)$$

where  $N_i$  represents the number of data points drawn by client  $c_i$  from  $\mathcal{D}_i$ . The central server and clients will collaboratively solve this optimization problem in an iterative manner, so we let  $W_t$  represent the model weights at time  $t$ . At the beginning of each round, the server selects  $N$  clients uniformly at random to participate. Each client downloads  $W_t$  and minimizes  $\mathcal{L}$  according to their own procedure and sends a model update to the central server. The server aggregates all the model updates to update the global weights.

*Remark.* When client memory is not an issue,  $\mathcal{W}$  is often parameterized by vectors  $w \in \mathbb{R}^d$ . However, for our setting, we are interested in matrices, due to their ubiquity in traditional machine learning settings and as we will see in Section 4, their amenability to parameterization via Count Sketches.

**Network Architectures.** We review the forward pass of two popular architectures: fully-connected networks and convolutional ResNets. Our description follows the notations of Du et al. (Du et al. 2019).

*Multilayer fully-connected networks:* Let  $\{W_t^\ell\}_{\ell=1}^L$  represent the weight matrices of our layers at time  $t$ , where  $L$  is the depth of the network. Let  $x \in \mathbb{R}^d$  be the input. We define the network prediction in a recursive manner. Let  $\sigma : \mathbb{R}^d \rightarrow \mathbb{R}^d$  represent a nonlinear activation function, and denote  $x^0 := x$ . We have that

$$x^\ell = \sigma(W_t^\ell x^{\ell-1}), \quad 1 \leq \ell \leq L-1$$

and the final prediction is  $\hat{y} = \mathbf{a}^\top x^L$ , where  $\mathbf{a} \in \mathbb{R}^d$  is the output layer. Here, we have omitted bias and regularization terms. The output  $\hat{y}$  is fed into  $\mathcal{L}$  where it is compared against the true label.

*Convolutional ResNet:* We will now describe the output of a typical convolutional ResNet architecture. We will intentionally avoid using any convolutional operators ( $*$ ) since we will be sketching along the input or output channel mode. Let  $x^0 \in \mathbb{R}^{s_0 \times p}$ , where  $s_0$  is the number of input channels and  $p$  is the number of pixels. We denote  $s^\ell = m$  as the number of channels and  $p$  as the number of pixels for all  $\ell \in [L]$ . For  $x^{\ell-1} \in \mathbb{R}^{s_{\ell-1} \times p}$ , we use an operator  $\phi_\ell(\cdot)$  to divide  $x^{\ell-1}$  into a stack of  $p$  patches. Each patch will have size  $qs_{\ell-1}$  which implies that  $\phi_\ell(x^{\ell-1}) \in \mathbb{R}^{qs_{\ell-1} \times p}$ . Let  $W_t^\ell \in \mathbb{R}^{s_\ell \times qs_{\ell-1}}$ . Similar to the fully-connected case, we define the layers recursively:

$$x^1 = \sqrt{\frac{c_\sigma}{m}} \sigma(W_t^1 \phi_0(x^0)),$$

$$x^\ell = x^{\ell-1} + \frac{c_{res}}{L\sqrt{m}} \sigma(W_t^\ell \phi_\ell(x^{\ell-1})), \quad 2 \leq \ell \leq L,$$

$0 < c_{res} < 1$ . The final output is  $\hat{y} = \langle W_t^L, x^L \rangle$ , where  $W_t^L \in \mathbb{R}^{m \times p}$  and  $\langle \cdot, \cdot \rangle$  is the Frobenius inner product.

**Count Sketch.** The crux of `ComFetch` is using the Count Sketch data structure to compress each layer’s weights. In this paper, we deal with networks whose weights are representable as matrices. Briefly, the Count Sketch data structure contains a collection of  $k$  pairwise-independent hashing maps  $h_i : [d] \rightarrow [c]$  for  $i \in [k]$ , each of which is paired with a sign map  $s_i : [d] \rightarrow \{\pm 1\}$ , for  $i \in [k]$ . Each hash function/sign map pair is used to project a  $d$ -dimensional vector  $x$  into a smaller  $c$ -dimensional space, which we refer to as a sketch. Through an “unsketch” procedure (detailed in Appendix A), we use the  $k$  sketches to create a  $d$ -dimensional approximation  $\hat{x}$  of  $x$ . To develop a sketch of a matrix, we apply a Count Sketch to each row of the weight matrix. Our method is generalizable to tensorial weights, but these require higher-order count sketches (HCS); we refer the reader to Appendix A for further treatment of HCS.

## 3 Related Work

**Network Compression.** A popular approach to network compression involves taking low-rank factorizations of the weight tensors (Oseledets 2011; Denil et al. 2013; Tai et al. 2015; Novikov et al. 2015). Often times, this will require learning the factors, which increases training overhead (Oseledets 2011; Denil et al. 2013) or increases the depth of the network (Tai et al. 2015), and computing exact tensor factorizations is known to be NP-hard (Gillis and Glineur 2011). `ComFetch` avoids these issues by relying on simple linear transformations of the original weights. Kasiviswanathan et al. (Kasiviswanathan, Narodytska, and Jin 2017) replace fully-connected and convolutional layers in a non-federated setting via sign sketches (Hadamard matrices). Their compressed CNNs perform worse than our federated learned models on CIFAR-10 (Krizhevsky, Nair, and Hinton) classification, cost more memory than our `ComFetch` to store,

and do not have convergence guarantees. Knowledge distillation (Hinton, Vinyals, and Dean 2015; Ba and Caruana 2013), quantization (Jacob et al. 2018), binarization (Hubara et al. 2016), Huffman coding (Han, Mao, and Dally 2015), and other similar techniques seek to gradually reduce the number of the parameters during training or compress the model post-training. In our scenario, the memory-constrained clients can never store the original architecture due to its size, and in most centralized federated learning settings, the server does not have access to the local client data (Kairouz et al. 2019), therefore rendering these techniques inapplicable. Hence, we opt for the popular Count Sketch compression scheme, which is data-oblivious.

**Communication-Efficient Federated Learning.** A practical assumption of centralized federated learning is that clients will be physically removed from the central server and communicating over unreliable wireless channels (Kairouz et al. 2019; Yang et al. 2018; Amiri and Gündüz 2020). Therefore, there has been significant interest in reducing the size of data communicated between the server and federated agents (Konečný et al. 2016). Ivkin et al. (Ivkin et al. 2019) suggested taking Count Sketches of the local gradients to reduce client update costs to great effect, but their algorithm `Sketched SGD` requires an extra round of communication with the server, which although is appropriate for their distributed single-machine setting, would fail in the general federated setting due to a lack of statefulness of the clients. Rothchild et al. (Rothchild et al. 2020) successfully eliminated the extra round of communication with their `FetchSGD` by taking several independent sketches of the gradients coupled with error feedback (Karimireddy et al. 2019) in the model update phase. `FetchSGD` only extracts the Top- $k$  components of the gradients to mitigate Count Sketch recovery error, similar to the `MISSION` algorithm of Aghazadeh et al. (Aghazadeh et al. 2018). While such methods successfully decrease upload communication costs, they do not address the client memory cost of hosting the global model, which could be a bottleneck for memory-constrained clients such as mobile devices. `Comfetch` simultaneously reduces local memory costs and reduces bidirectional communication costs for free by having clients train on smaller models.

## 4 Comfetch

We propose Algorithm 1, `Comfetch`, to minimize the aggregated loss function (equation 1) of a large network on memory-constrained devices. Algorithm 1 uses only a single sketch, but a multi-sketch version is needed for convergence Theorem 1. Due to the complexity of the multi-sketch algorithm and experimentally-observed efficacy of the single-sketch scheme, we reserve all discussion of multi-sketch `Comfetch` to Appendix C, and assume a single Count Sketch is used for all weight compressions for the remainder of this section.

We use a sketch-unsketch paradigm  $W_t^\ell \rightarrow H^{\ell\top} H^\ell W_t^\ell$ , where  $H^\ell \in \mathbb{R}^{d \times c}$  is a randomly drawn Count Sketch matrix to approximate each weight  $W_t^\ell \in \mathbb{R}^{d \times d}$ , with  $c \ll d$ . We require the client to store only a hash-function  $h^\ell \in \mathbb{R}^d$  associated to  $H^\ell$  and the sketched weight  $H^\ell W_t^\ell$ , thus reducing

the memory footprint of storing each layer from  $\mathcal{O}(d^2)$  to  $\mathcal{O}((c+1)d)$ . (As an abuse of notation, we use  $h^\ell$  and  $H^\ell$  interchangeably, since one may infer  $H^\ell$  from  $h^\ell$ , the latter of which we will actually transmit in implementation since it is cheaper to do so.) We design a mechanism for the central controller to aggregate model updates from the clients and backpropagate the sketched model parameters. The algorithm follows a typical structure of a federated learning algorithm: *model transmission and download*, *client update*, and *model update*. This process is repeated over  $T$  iterations. We will describe each phases in detail for a fixed weight. For simplicity of notations, we assume that  $W_t^\ell \in \mathbb{R}^{d \times d}$ .

---

### Algorithm 1: `Comfetch` (Single Sketch)

---

**Require:** initial weights  $\{W_0^\ell\}_{\ell=1}^L$ , learning rate  $\eta$ , number of iterations  $T$ , momentum parameter  $\rho$ , batch size  $M$  of data, batch size  $N$  of clients  
 Init momentum term  $\{u_0^\ell = 0\}_{\ell=1}^L$   
 2: Init error accumulation term  $e_0 = 0$   
**for**  $t = 1, 2, \dots, T$  **do**  
 4:   Init weight sketches  $\{H^{\ell\top}, H^\ell W_t^\ell\}_{\ell=1}^L$   
    Uniformly select at random  $N$  clients  $c_1, c_2, \dots, c_N$   
 6:   **loop** {in parallel on clients  $\{c_i\}_{i=1}^N$ }  
    **for**  $\ell = 1, 2, \dots, L$  **do**  
 8:     Download weight sketches  $\{H^{\ell\top}, H^\ell W_t^\ell\}_{\ell=1}^L$   
    Compute grads  $g_i^\ell = \nabla_{H^\ell w_i^\ell} \mathcal{L}(\hat{W}_t^\ell, z \sim \mathcal{D}_i)$   
 10:      $\triangleright \hat{W}_t^\ell = H^{\ell\top} H^\ell W_t^\ell$   
    Send  $\{g_i^\ell\}_{\ell=1}^L$  to Central Server  
 12:   **end loop**  
   **for**  $\ell = 1, 2, \dots, L$  **do**  
 14:     Aggregate restored gradients:  $g^\ell = \frac{1}{N} \sum_{i=1}^N g_i^\ell$   
    Update momentum:  $u_t^\ell = \rho u_{t-1}^\ell + g^\ell$   
 16:     Update error feedback:  $e_t^\ell = \eta u_t^\ell + e_t^\ell$   
    Approximate gradient:  $\Delta_t = \text{Top-}k(e_t^\ell)$   
 18:     Error accumulation:  $e_{t+1}^\ell = e_t^\ell - \Delta_t$   
    Update weight:  $W_{t+1}^\ell = W_t^\ell - \Delta_t$   
**return**  $\{W_T^\ell\}_{\ell=1}^L$

---

### 4.1 Model Transmission and Download

At iteration  $t$ , the central server first prepares the global model for the transmission by sketching down all the current weights  $\{W_t^\ell\}_{\ell=1}^L$ , via Count Sketch matrices  $H^\ell \in \mathbb{R}^{c \times d}$ , where  $c \ll d$  is referred to as the sketching length. These matrices are described in Appendix A. We assume that our layers are either convolutional or fully-connected as described in Section 2, and for simplicity, that all  $W_t^\ell$  are of size  $d \times d$ , but they can be rectangular in practice. For each weight  $W_t^\ell$ , the server randomly draws a Count Sketch matrix  $H^\ell$ . The server transmits  $\{(H^{\ell\top}, H^\ell W_t^\ell)\}_{\ell=1}^L$  to  $N$  clients drawn uniformly at random, who then download the sketched parameters into local memory.

**Cost Complexity.** Note that any  $H^\ell$  bijectively corresponds to a hash function  $h^\ell : d \rightarrow c$  which is representable as a length  $d$  vector, but it is cheaper to store/transmit  $h^\ell$ . Hence, in practice, the central server will transmit

$\{(h^\ell, H_i^\ell W_t^\ell)\}_{\ell=1}^L$ , for a total local memory and transmission cost of  $\mathcal{O}((c+1)d)$ , which is far less than the usual  $\mathcal{O}(d^2)$  cost of transmission and storage.

*Remark.* Note that the sketches are linear transformations of the weights from the left, but two-sided sketching for further compression also possible, which we detail in Appendix A.

## 4.2 Client Update

The client  $C_i$  will now conduct a single round of training on the sketched network parameters using local data. In practice, the client distributions  $\mathcal{D}_i$  will be finite and small (Kairouz et al. 2019), so we assume that the client is taking the full gradient with respect to the weights, but the algorithm generalizes to stochastic gradients as well.

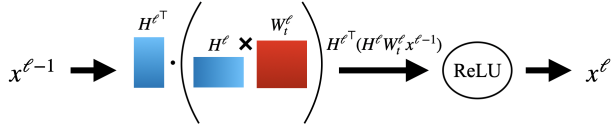


**Figure 1:** The forward pass of an FC layer.

**Forward pass.** Assume there are  $L$  weights. Following the notations described in Section 2, the forward pass of a fully-connected (FC) layer is

$$x^\ell = \sigma(H^{\ell\top}(H^\ell W_t^\ell x^{\ell-1})), \quad (2)$$

for  $1 \leq \ell \leq L-1$  and the final output is  $\hat{y} = \mathbf{a}^\top x^L$ . Similarly, for a convolutional ResNet, we have that

$$x^1 = \sqrt{\frac{c_\sigma}{m}} \sigma\left(H^1 \top (H^1 W^1 \phi_1(x^0))\right), \quad (3)$$

$$x^\ell = x^{\ell-1} + \frac{c_{res}}{L\sqrt{m}} \sigma\left(H^\ell \top (H^\ell W^\ell \phi_\ell(x^{\ell-1}))\right), \quad (4)$$

for  $2 \leq \ell \leq L$  and the final output is  $\hat{y} = \langle W^L, x^L \rangle$ , where  $W^L \in \mathbb{R}^{m \times p}$ .

**Cost Complexity.** Each sketched weight costs the client  $\mathcal{O}(cd)$  to locally store which is an improvement over storing the original weight which costs  $\mathcal{O}(d^2)$ .

*Remark 1:* We never store or directly compute a  $d \times d$  weight matrix at any stage. As emphasized by parenthetical grouping, in the case of an fully-connected layer, we compute  $H^\ell W_t^\ell x^{\ell-1}$ , followed by a multiplication on the left by  $H^{\ell\top}$ , thereby only storing vectors of dimension  $d$ . Similarly, for a convolutional layer, we first compute  $H^\ell W^\ell \phi_\ell(x^{\ell-1})$ , followed by a multiplication on the left by  $H^{\ell\top}$ , which similarly does not require storage of a full weight.

*Remark 2:* In the convolutional case, where the inputs between layers are matrices,  $H^\ell W^\ell \phi_\ell(x^{\ell-1})$  can be regarded as a higher-order count sketch (HCS) of  $W^\ell \phi_\ell(x^{\ell-1})$  as described in Appendix A.

*Remark 3:* We do not sketch the final weight  $W_L$  of convolutional ResNet since  $x^L$  is a vector of size equal to the number of classes.

**Backward pass.** In order to compute the gradient, we must first clearly define the weights of the client networks. We have  $H^{\ell\top} H^\ell W_t^\ell x^{\ell-1}$  and  $H^\ell W^\ell \phi_\ell(x^{\ell-1})$  in the fully-connected and convolutional layers, respectively. Therefore, we can represent each sketched weight as  $R^\ell W_t^\ell$  where  $R^\ell = H^{\ell\top} H^\ell$ , so our sketches are simple linear transformations of the original weights. For further notational convenience, we denote  $\hat{W}_t^\ell \triangleq R^\ell W_t^\ell$ . Now that we have defined the weights of our client models, we may now take gradients. The server will want to receive  $\frac{\partial \mathcal{L}(\hat{W}_t^\ell, z)}{\partial W_t^\ell}$  as an approximation of  $\frac{\partial \mathcal{L}(W_t^\ell, z)}{\partial W_t^\ell}$ , but the client will not want to store  $\frac{\partial \mathcal{L}(\hat{W}_t^\ell, z)}{\partial W_t^\ell}$ , since it is of size  $d \times d$ . We will want to transmit a  $\mathcal{O}(c \times d)$  packet of data which will allow the server to compute  $\frac{\partial \mathcal{L}(\hat{W}_t^\ell, z)}{\partial W_t^\ell}$ . We take advantage of the chain rule of multi-variable calculus. We have that,

$$\frac{\partial \mathcal{L}(\hat{W}_t^\ell, z)}{\partial W_t^\ell} = \sum_{i=1}^k \frac{\partial \mathcal{L}(\hat{W}_t^\ell, z)}{\partial H^\ell W_t^\ell} \frac{\partial H^\ell W_t^\ell}{\partial W_t^\ell}. \quad (5)$$

Since the server is capable of computing  $\frac{\partial H^\ell W_t^\ell}{\partial W_t^\ell} = H^\ell$ , the client need only upload

$$g_i^\ell \triangleq \nabla_{H^\ell W_t^\ell} \mathcal{L}(\hat{W}_t^\ell, z) \in \mathbb{R}^{c \times d}. \quad (6)$$

**Cost Complexity.** Each  $g_i^\ell$  costs  $\mathcal{O}(cd)$  to store and transmit, which is a strong improvement over the usual uplink cost of  $\mathcal{O}(d^2)$  and even cheaper than the sketched storage cost of  $\mathcal{O}((c+1)d)$ .

*Remark.* The client will never directly compute  $g_i^\ell \in \mathbb{R}^{d \times d}$ . The purpose of equation (5) is to illustrate that we may take a well-defined gradient. In practice, the client will use an autograd-like library.

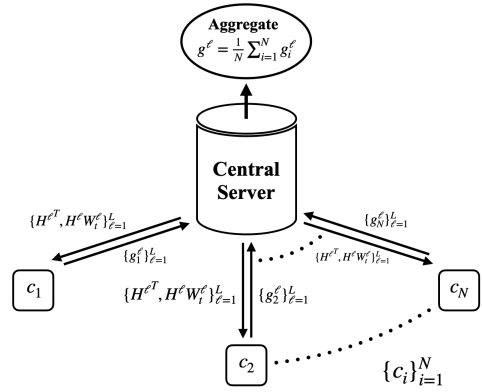


**Figure 2:** ComFetch Communication. A high-level depiction of data being sent over the edge in ComFetch. The server communicates sketched weights to the client and the client uploads local gradients with respect to the sketched weights.

## 4.3 Model Update

The Central Server aggregates the  $\{g_i^\ell\}_{\ell=1}^L$  across all clients  $c_i$  for  $i \in [N]$ . The server computes a one-shot average over

the approximate gradients,  $g^\ell = \frac{1}{N} H^{\ell \top} \sum_{i=1}^N g_i^\ell$ .

The remainder of the model update is an SGD-like procedure which follows the error-feedback and momentum scheme of `FetchSGD` (Rothchild et al. 2020). The error-feedback term  $e_t$  allows for the correction of error associated with our gradient approximations  $g^\ell$ . Specifically, we are correcting the error associated with using  $\nabla_{W_t^\ell} f(R^\ell W_t^\ell)$  as an approximation of  $\nabla f(W_t^\ell)$ . Once we form the full error term  $e_t$ , we take the Top- $k$  components (in absolute magnitude) of it, which we expect to be relatively undiluted by the approximation error, to form  $\Delta_t$ . We have that  $\Delta_t$  is our error-corrected gradient approximation with a momentum term already baked into it. (The momentum term  $u_t$  is common to SGD-variants in the non-federated setting, the benefits of which are discussed by Sutskever et al. (Hinton, Vinyals, and Dean 2015).) This  $\Delta_t$  will help us mimic stochastic gradient descent, as shown in Line 18 of Algorithm 1. The reader is encouraged to consult the work of Karimireddy et al. and Stich et al. for further details on error-feedback for SGD-like methods (Karimireddy et al. 2019; Stich, Cordonnier, and Jaggi 2018).

## 5 Convergence Analysis

In this section, we provide a convergence result for `ComFetch` and analysis of the error between the prediction of a sketched network versus the original network. For all results,  $\|\cdot\|$  refers to the  $\ell_2$  norm. We first state our result and then outline our assumptions. Proof is in Appendix B.

**Theorem 1.** *Under Assumptions 1-6, multi-sketch `ComFetch`, with step size  $\eta = \frac{c^8(1-\rho)}{2d^8 L^2 \sqrt{T}}$ , in  $T$  iterations, returns  $\{W_t^\ell\}_{i=1}^T$  such that  $\min_{t=1 \dots T} \|\nabla_{W_t^\ell} f(\hat{W}_t^\ell)\|^2 \rightarrow 0$  as  $T \rightarrow \infty$  with probability at least  $(1 - \delta)$  over the sketching randomness. Furthermore, let  $A = \frac{d^8 L^2 (f(W_0^\ell) - f^*)}{c^8 \sqrt{T}}$ ,  $B = \frac{4(1-\epsilon)G^2}{T^2 \epsilon^2 (1-\rho)^3}$ ,  $C = \frac{c^4(1+c)^2 B^2}{d^4 T} + \frac{G^2}{T}$ . Then*

$$\min_{t=1 \dots T} \|\nabla_{W_t^\ell} f(\hat{W}_t^\ell)\|^2 = \Omega(A + B + C), \quad (7)$$

where  $k = \Omega(\log \frac{d}{\delta})$  independent sketches are taken of  $W_t^\ell$  with  $c = \Omega(B^2/\epsilon^2)$  sketching length.

*Remark 1.* The result is a statement about the convergence of one particular weight. For full convergence of all  $\ell$  weights, our probability decreases to  $(1 - \delta)^L$ . However, the sketching randomness is independent between rounds.

*Remark 2.* The theory is more restrictive than our empirical results, which is often the case with sketching compression schemes, as the classical sketching concentration bounds are ensured via multiple sketches. In particular, using only a single sketch works well as shown in Section 6. Furthermore, the sketched weights were heterogeneous across clients in the multi-sketch experiments, violating assumption 6).

*Remark 3.* The prescribed number of independent sketches and sketch length are specific to the guarantees of the higher order count sketch (Shi and Anandkumar 2019).

**Assumption 1** ( $L$ -Smooth). *The objective function  $f(W)$  in equation 1 is  $L$ -smooth. That is, for all  $x, y \in \mathbb{R}^{d \times d}$  we have*

that,

$$\|\nabla f(x) - \nabla f(y)\| \leq L\|x - y\|. \quad (8)$$

**Assumption 2** (Unbiased and Bounded). *All stochastic gradients  $g_t$  of  $f(W_t)$  are unbiased and bounded,*

$$\mathbb{E}g_t = \nabla f(W_t^\ell) \text{ and } \mathbb{E}\|g_t\|^2 \leq G^2. \quad (9)$$

Assumptions 1-2 are standard to convergence proofs of SGD-like algorithms, including those of a federated nature (Karimireddy et al. 2019; Nemirovski et al. 2009; Ivkin et al. 2019; Shalev-Shwartz et al. 2011; Rothchild et al. 2020).

**Assumption 3** (Heavy Hitters). *In the notation of Algorithm 1, let  $\{W_t^\ell\}_{t=1}^T$  be the sequence of model weights of the  $\ell^{\text{th}}$  layer generated by the `ComFetch`. There exists a constant  $\epsilon$  such that for all  $t \in [T]$ , the approximate gradient with momentum  $z_t^\ell := \eta(\rho u_{t-1}^\ell + g_{t-1}^\ell) + e_{t-1}^\ell$  contains at least one coordinate  $i$  such that  $(z_t^\ell)_i^2 \geq \epsilon\|z_t^\ell\|^2$ . Furthermore, there exists a constant  $c$  such that for any given weight  $W_t^\ell$ , there exists a coordinate  $j$  with  $(W_t^\ell)_j^2 \geq (1/c)\|W_t^\ell\|^2$ . These coordinates are referred to as heavy hitters (Alon, Matias, and Szegedy 1999).*

Assumption 3 was first suggested in the convergence theorem of `FetchSGD` to ensure successful error-feedback (Rothchild et al. 2020), and since the model update of `ComFetch` adopts the error-feedback procedure of `FetchSGD`, we also require it. The difference is that `FetchSGD` only needs a heavy hitter for the approximate gradient with momentum  $z_t^\ell$ , while we require a heavy hitter for every weight matrix.

**Assumption 4** (Bounded Weights). *The norms of our weights are uniformly bounded. That is, there exists a  $B$  such that  $\|W_t^\ell\| \leq B^2$  for all  $t \in [T]$  and  $\ell \in [L]$ .*

Assumption 4 is needed to achieve a bound on the  $\ell_2$ -norm of a higher-order count sketch (see Appendix A).

**Assumption 5** (Single Point Training). *We assume that each client  $c_i$  only draws and trains on a single sample from their local distribution  $\mathcal{D}_i$  at each iteration.*

In practice, federated agents will often be expected to train on small datasets, either due to limited local data or to expedite training while on a weak, unreliable channel (Kairouz et al. 2019). This will ensure that we may represent our sketched weights uniquely as  $R_i^\ell W_t^\ell$ , where  $R_i^\ell$  is the recovery matrix associated with the single sample.

**Assumption 6** (Client Model Homogeneity). <sup>1</sup> *For all  $t \in [T]$  and any two clients  $c_i, c_j$  where  $i \neq j$ ,  $R_i^\ell = R_j^\ell$  for all  $\ell \in [L]$  as in Appendix C, where  $R_i^\ell, R_j^\ell \in \mathbb{R}^{d \times d}$  are the recovery matrices of  $W_t^\ell x^{\ell-1}$  on clients  $i$  and  $j$ , which are well-defined since we train on a single point by Assumption 5. Therefore,  $R_i^\ell W_t^\ell = R_j^\ell W_t^\ell$ , so the intra-layer weights are homogeneous between client models.*

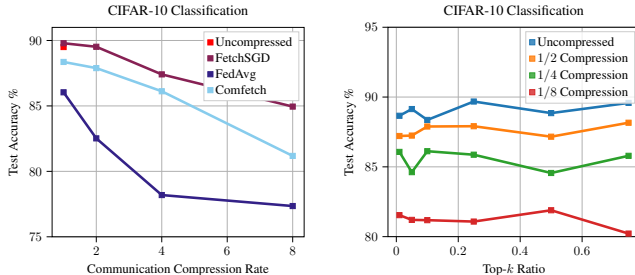
Assumption 6 is specific to our setting, but also required to ensure that our weights are homogeneous between client models, which is necessitated by definition of the objective function  $f(W)$ . It is automatically satisfied in the case of single sketch ( $k = 1$ ) compression. Intuitively, Assumption 6 implies that all the samples have similar features.

<sup>1</sup>Assumption 6 uses concepts specific to the multi-sketch `ComFetch` which are detailed in Appendix C.

## 6 Experiments

**Baselines.** No existing method addresses the memory constraint problem, which is the major contribution of `Comfetch`, thus there are no valid baselines except for smaller global models. While no previous federated method has explored deploying compressed models on the client side while the global model is large, we still compare our performance against the state-of-the-art `FetchSGD` (Rothchild et al. 2020) and also `FedAvg` (McMahan et al. 2017) for reference. `Comfetch` has an important advantage over existing methods with its capability of performing network operations in a compressed form. On the other hand, while `FetchSGD` is able to achieve great communication reduction rate during network training, it requires each client to store the full network weights, even though the client might only perform a few iterations of training. This property might be sub-optimal when the client’s memory resources are limited.

Since `Comfetch` is the first method to train a large network using memory-constrained clients, it inevitably suffers from some performance loss compared to other methods that allow clients to host large models. Nevertheless, we still investigate the communication-efficiency of `Comfetch` compared against `FetchSGD` (a state-of-the-art communication efficient method) and `FedAvg` (a popular baseline).



(a) Accuracy vs Compression (b) Accuracy vs Top- $k$  Ratio

**Figure 3:** Test accuracy achieved on CIFAR-10 classification. In (a), we emphasize that **under the same communication compression CR (the horizontal axis), the reported performance achieved by `Comfetch` requires  $1/\text{CR}$  times smaller client memory footprint than `FetchSGD`**. `FetchSGD` only compresses the network weights during communication, but each client still needs to decompress the entire network locally to perform training. So our constructions of the baselines are inherently advantaged against our `Comfetch`.

**Datasets and Setup.** We test `Comfetch` on an image classification task and a part of speech prediction language task. We evaluate `Comfetch`’s performance on two prevalent architectures: recurrent neural networks (RNN) for the language task and convolution neural networks (CNN) for the image task. To evaluate our method’s performance on language data in RNNs such as LSTMs (Hochreiter and Schmidhuber 1997), we use MNLI (Williams, Nangia, and Bowman 2017), a large corpora with 549k sentence pairs. We implement a naive LSTM to predict part of speech tagging for sentences in MNLI. For training, we use 5k sentences. The language task experiments are run on an Intel Core i7-8700K machine with NVIDIA GeForce RTX 2070 Super and 16 GiB RAM. To evaluate our method’s perfor-

Method	Relative Client Mem. Cost	Relative Bandwidth Cost	Relative Global Model Size allowed	Test Acc (%)
FedAvg	1	1	1	86.04
FetchSGD	1	1	1	<b>88.72</b>
Comfetch	1	1	1	88.36
<hr/>				
FedAvg	1/2	1/2	1/2	75.38
FetchSGD	1/2	1/2	1/2	74.26
Comfetch	1/2	1/2	1	<b>87.89</b>
<hr/>				
FedAvg	1/4	1/4	1/4	73.34
FetchSGD	1/4	1/4	1/4	74.03
Comfetch	1/4	1/4	1	<b>86.12</b>
<hr/>				
FedAvg	1/8	1/8	1/8	72.40
FetchSGD	1/8	1/8	1/8	71.67
Comfetch	1/8	1/8	1	<b>81.18</b>

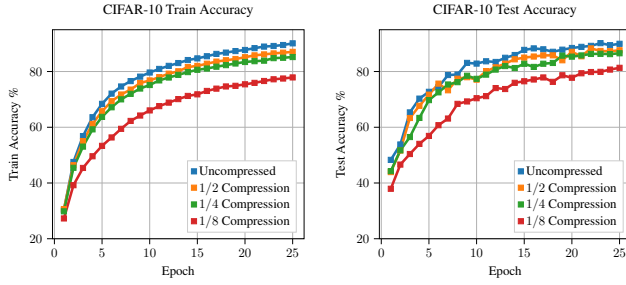
**Table 1:** Test accuracy under different memory footprints in clients for the CIFAR-10 (Krizhevsky, Nair, and Hinton) image classification task. `Comfetch` maintains a large and powerful global model under communication compression and client memory compression, whereas the baseline requires the global model to be smaller to obtain the same communication and client memory efficiency. Since `FedAvg` and `FetchSGD` cannot achieve any memory compression by design, we reduce the global network layer width to achieve a de facto reduction in memory. While `FetchSGD` focuses on bandwidth compression, we obtain its best-case performance by setting the bandwidth compression ratio as 1. The results indicate that our methods achieve competitive performance when the bandwidth and client memory are limited.

mance on image classification via CNNs such as ResNet (He et al. 2016), we use CIFAR-10 (Krizhevsky 2009), a benchmark computer vision dataset with 60,000  $32 \times 32$  color images. The CIFAR-10 experiments are run on a cloud cluster with a NVIDIA Tesla T4 and 16 GiB RAM.

**Hyperparameters.** We implement `FetchSGD` (following (Rothchild et al. 2020)) and `FedAvg` (following (McMahan et al. 2017)) to distribute the input images/texts to clients, and report accuracy on the test dataset. In the CIFAR-10 image classification task, unless otherwise noted, we set  $k$  equal to 10% of the total parameters. The `FetchSGD` results are similarly obtained to ensure comparability. We set the mini-batch size of each client to be 16, and keep the learning rate constant at 0.001. We train all models for 25 epochs. For the part of speech prediction task, we set the default  $k = 1$ , learning rate equal to 0.01, batch size equal to 1, and all models are trained for 5 epochs.

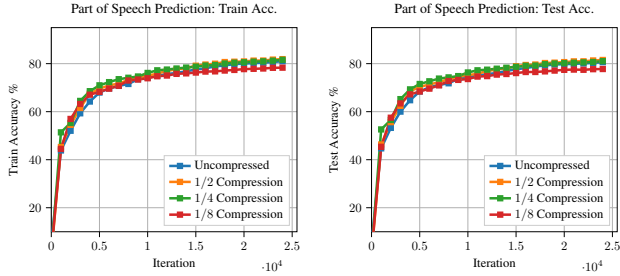
### 6.1 Performance under Limited Communication Bandwidth

**`Comfetch` is performance-preserving in CNNs and RNNs without the requirement of full model-hosting on clients.** To simulate limited communication compression in the other methods, we decrease the number of allowable iterations in `FedAvg` and compress the outgoing gradients of `FetchSGD`. In both the image (Figure 3) and language (Figure 4) task, we are training on significantly compressed models while still maintaining competitiveness. We also notice that the baseline method `FedAvg` has inferior performance, mirroring the observations of Rothchild et al. (2020).



(a) Train Accuracy

(b) Test Accuracy



(c) Train Accuracy

(d) Test Accuracy

**Figure 4:** Test accuracy convergence of `Comfetch` under varying compression rates. (a)-(b) correspond to the CIFAR-10 (Krizhevsky, Nair, and Hinton) image classification, while (c)-(d) correspond to a part of speech prediction on MNL (Williams, Nangia, and Bowman 2017) sentences. In these experiments, only a single sketch is used. Similar accuracy with 1) different `Comfetch` compression rates suggests that our method retains the expressive power of the model while reducing the parameter counts, and 2) in the MLNI language task may be the result of task easiness.

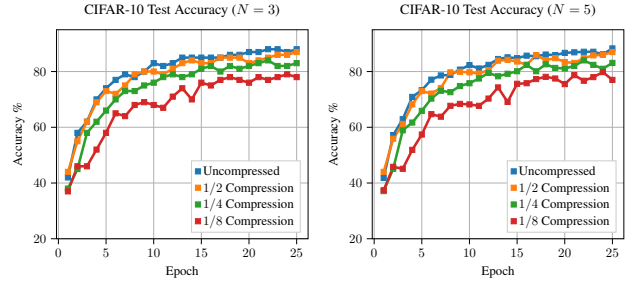
## 6.2 Performance under Limited Local Client Memory

In Table 1, we note that `Comfetch` achieves better test accuracies than baselines when clients are operating under lower local memory budgets and communication bandwidth. Under the same constraints, `Comfetch` allows for training of a larger global model and thus achieves better performance. `FetchSGD` only focuses on compressing the bandwidth cost of gradient communications, while requiring the full network weights to be stored in the client devices. According to additional data in Appendix D, `Comfetch` is able to achieve competitive performance against existing methods while significantly reducing the memory footprint required on the client devices.

## 6.3 Ablation Studies of Various Parameters

**Effects of the Top- $k$  ratio and compression rates.** As shown in Figure 3(b), the performance of `Comfetch` is fairly consistent under different  $k$  values for a Top- $k$  recovery scheme, across various compression rates. We show convergence plots in Figure 4 under different compression rates.

**Effects of using multiple sketches.** We perform further ablation studies on the effect of the number of sketches on network performance, the results of which are presented in Figure 5 and Figure 6. Multi-sketch `Comfetch` is thoroughly discussed in Appendix C. Our results indicate that, in practice, `Comfetch` can be reliably deployed for network training using only 1 sketch per weight, which is ideal for re-



(a) Accuracy using 3 sketches

(b) Accuracy using 5 sketches

**Figure 5:** Effects of the number of sketches used on CIFAR-10 classification. We send  $N$  different sketches to the clients at each iteration of training. We observe that performance does not degrade even when only 1 sketch is used across all clients, suggesting that in practice we could avoid sending multiple sketches to reduce bandwidth and memory costs while maintaining training robustness.

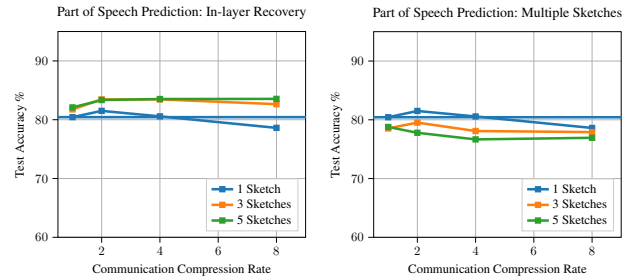


**Figure 6:** Effects of the number of sketches used on part of speech taggings for MNL (Williams, Nangia, and Bowman 2017) sentences. We test in-layer recovery by taking the median of the result of multiple unsketches (left), and varying the number of clients (right). We find that 1) using multiple sketches to perform in-layer recovery improves accuracy, and 2) the performance of our algorithm does not significantly change with the number of sketches.

ducing training overhead, communication costs, and memory costs.

## 7 Conclusion

In this work, we present a federated learning algorithm `Comfetch` for training large networks on memory-constrained clients. In our scheme, the central server parameterizes the global model via Count Sketches of the weight matrices, significantly reducing storage costs. While using multiple Count Sketches per weight provides us with a convergence guarantee, we experimentally demonstrate that using only a single sketch is performance-preserving. To the best of our knowledge, we are the first to suggest a federated learning algorithm for model compression.

The limitations of `Comfetch` motivate future directions. We note that theory developed in Section 5 concurs with the results of the multi-sketch experiments provided in Figures 5 and 6, but does not predict the success of single-sketch `Comfetch` which we observe in Figure 4. Structurally-aware sketches (Zhang et al. 2020; Chen and Zhang 2016) or oblivious sketches (Ahle et al. 2020) with strong guarantees may hold the key to a guaranteed one-sketch scheme.

## Acknowledgements

Rabbani is supported in part by NSF award DGE-1632976. Huang is supported by National Science Foundation IIS-1850220 CRII Award 030742-00001, DOD-DARPA-Defense Advanced Research Projects Agency Guaranteeing AI Robustness against Deception (GARD), and Adobe, Capital One and JP Morgan faculty fellowships.

## References

- Aghazadeh, A.; Spring, R.; Lejeune, D.; Dasarathy, G.; Shrivastava, A.; et al. 2018. Mission: Ultra large-scale feature selection using count-sketches. In *International Conference on Machine Learning*, 80–88. PMLR.
- Ahle, T. D.; Kapralov, M.; Knudsen, J. B.; Pagh, R.; Velingker, A.; Woodruff, D. P.; and Zandieh, A. 2020. Oblivious sketching of high-degree polynomial kernels. In *Proceedings of the Fourteenth Annual ACM-SIAM Symposium on Discrete Algorithms*, 141–160. SIAM.
- Alon, N.; Matias, Y.; and Szegedy, M. 1999. The space complexity of approximating the frequency moments. *Journal of Computer and system sciences*, 58(1): 137–147.
- Amiri, M. M.; and Gündüz, D. 2020. Federated learning over wireless fading channels. *IEEE Transactions on Wireless Communications*, 19(5): 3546–3557.
- Ba, L. J.; and Caruana, R. 2013. Do deep nets really need to be deep? *arXiv preprint arXiv:1312.6184*.
- Brisimi, T. S.; Chen, R.; Mela, T.; Olshevsky, A.; Paschalidis, I. C.; and Shi, W. 2018. Federated learning of predictive models from federated electronic health records. *International journal of medical informatics*, 112: 59–67.
- Charikar, M.; Chen, K.; and Farach-Colton, M. 2002. Finding frequent items in data streams. In *International Colloquium on Automata, Languages, and Programming*, 693–703. Springer.
- Chen, J.; and Zhang, Q. 2016. Bias-aware sketches. *arXiv preprint arXiv:1610.07718*.
- Cormode, G.; and Muthukrishnan, S. 2005. An improved data stream summary: the count-min sketch and its applications. *Journal of Algorithms*, 55(1): 58–75.
- Deng, Y. 2019. Deep learning on mobile devices: a review. In *Mobile Multimedia/Image Processing, Security, and Applications 2019*, volume 10993, 109930A. International Society for Optics and Photonics.
- Denil, M.; Shakibi, B.; Dinh, L.; Ranzato, M.; and De Freitas, N. 2013. Predicting parameters in deep learning. *arXiv preprint arXiv:1306.0543*.
- Du, S.; Lee, J.; Li, H.; Wang, L.; and Zhai, X. 2019. Gradient descent finds global minima of deep neural networks. In *International Conference on Machine Learning*, 1675–1685. PMLR.
- Gillis, N.; and Glineur, F. 2011. Low-rank matrix approximation with weights or missing data is NP-hard. *SIAM Journal on Matrix Analysis and Applications*, 32(4): 1149–1165.
- Haddadpour, F.; Kamani, M. M.; Mokhtari, A.; and Mahdavi, M. 2021. Federated learning with compression: Unified analysis and sharp guarantees. In *International Conference on Artificial Intelligence and Statistics*, 2350–2358. PMLR.
- Han, S.; Mao, H.; and Dally, W. J. 2015. Deep compression: Compressing deep neural networks with pruning, trained quantization and Huffman coding. *arXiv preprint arXiv:1510.00149*.



- He, K.; Zhang, X.; Ren, S.; and Sun, J. 2016. Deep Residual Learning for Image Recognition. *2016 IEEE Conference on Computer Vision and Pattern Recognition (CVPR)*, 770–778.
- Hinton, G.; Vinyals, O.; and Dean, J. 2015. Distilling the knowledge in a neural network. *arXiv preprint arXiv:1503.02531*.
- Hochreiter, S.; and Schmidhuber, J. 1997. Long short-term memory. *Neural computation*, 9(8): 1735–1780.
- Hubara, I.; Courbariaux, M.; Soudry, D.; El-Yaniv, R.; and Bengio, Y. 2016. Binarized neural networks. In *Proceedings of the 30th International Conference on Neural Information Processing Systems*, 4114–4122.
- Ivkin, N.; Rothchild, D.; Ullah, E.; Braverman, V.; Stoica, I.; and Arora, R. 2019. Communication-efficient distributed SGD with sketching. *arXiv preprint arXiv:1903.04488*.
- Jacob, B.; Kligys, S.; Chen, B.; Zhu, M.; Tang, M.; Howard, A.; Adam, H.; and Kalenichenko, D. 2018. Quantization and training of neural networks for efficient integer-arithmetic-only inference. In *Proceedings of the IEEE Conference on Computer Vision and Pattern Recognition*, 2704–2713.
- Jiang, D.; Song, Y.; Tong, Y.; Wu, X.; Zhao, W.; Xu, Q.; and Yang, Q. 2019. Federated topic modeling. In *Proceedings of the 28th ACM International Conference on Information and Knowledge Management*, 1071–1080.
- Jin, R.; Kolda, T. G.; and Ward, R. 2019. Faster Johnson-Lindenstrauss transforms via kronecker products. *arXiv preprint arXiv:1909.04801*.
- Kairouz, P.; McMahan, H. B.; Avent, B.; Bellet, A.; Bennis, M.; Bhagoji, A. N.; Bonawitz, K.; Charles, Z.; Cormode, G.; Cummings, R.; et al. 2019. Advances and open problems in federated learning. *arXiv preprint arXiv:1912.04977*.
- Karimireddy, S. P.; Rebjock, Q.; Stich, S.; and Jaggi, M. 2019. Error feedback fixes signsgd and other gradient compression schemes. In *International Conference on Machine Learning*, 3252–3261. PMLR.
- Kasiviswanathan, S. P.; Narodytska, N.; and Jin, H. 2017. Deep neural network approximation using tensor sketching. *arXiv preprint arXiv:1710.07850*.
- Konečný, J.; McMahan, H. B.; Yu, F. X.; Richtárik, P.; Suresh, A. T.; and Bacon, D. 2016. Federated learning: Strategies for improving communication efficiency. *arXiv preprint arXiv:1610.05492*.
- Krizhevsky, A. 2009. Learning Multiple Layers of Features from Tiny Images.
- Krizhevsky, A.; Nair, V.; and Hinton, G. ????. CIFAR-10 (Canadian Institute for Advanced Research).
- McMahan, B.; Moore, E.; Ramage, D.; Hampson, S.; and y Arcas, B. A. 2017. Communication-efficient learning of deep networks from decentralized data. In *Artificial Intelligence and Statistics*, 1273–1282. PMLR.
- Nemirovski, A.; Juditsky, A.; Lan, G.; and Shapiro, A. 2009. Robust stochastic approximation approach to stochastic programming. *SIAM Journal on optimization*, 19(4): 1574–1609.
- Novikov, A.; Podoprikin, D.; Osokin, A.; and Vetrov, D. 2015. Tensorizing neural networks. *arXiv preprint arXiv:1509.06569*.
- Oseledets, I. V. 2011. Tensor-train decomposition. *SIAM Journal on Scientific Computing*, 33(5): 2295–2317.
- Pham, N.; and Pagh, R. 2013. Fast and scalable polynomial kernels via explicit feature maps. In *Proceedings of the 19th ACM SIGKDD international conference on Knowledge discovery and data mining*, 239–247.
- Pokhrel, S. R. 2020. Federated learning meets blockchain at 6G edge: A drone-assisted networking for disaster response. In *Proceedings of the 2nd ACM MobiCom Workshop on Drone Assisted Wireless Communications for 5G and Beyond*, 49–54.
- Pokhrel, S. R.; and Choi, J. 2020. Federated learning with blockchain for autonomous vehicles: Analysis and design challenges. *IEEE Transactions on Communications*, 68(8): 4734–4746.
- Rothchild, D.; Panda, A.; Ullah, E.; Ivkin, N.; Stoica, I.; Braverman, V.; Gonzalez, J.; and Arora, R. 2020. Fetchsgd: Communication-efficient federated learning with sketching. In *International Conference on Machine Learning*, 8253–8265. PMLR.
- Shalev-Shwartz, S.; Singer, Y.; Srebro, N.; and Cotter, A. 2011. Pegasos: Primal estimated sub-gradient solver for svm. *Mathematical programming*, 127(1): 3–30.
- Sherstinsky, A. 2020. Fundamentals of recurrent neural network (RNN) and long short-term memory (LSTM) network. *Physica D: Nonlinear Phenomena*, 404: 132306.
- Shi, Y.; and Anandkumar, A. 2019. Higher-order Count Sketch: Dimensionality Reduction That Retains Efficient Tensor Operations. *arXiv preprint arXiv:1901.11261*.
- Spring, R.; Kyrillidis, A.; Mohan, V.; and Shrivastava, A. 2019. Compressing gradient optimizers via count-sketches. In *International Conference on Machine Learning*, 5946–5955. PMLR.
- Stich, S. U.; Cordonnier, J.-B.; and Jaggi, M. 2018. Sparsified SGD with memory. *arXiv preprint arXiv:1809.07599*.
- Tai, C.; Xiao, T.; Zhang, Y.; Wang, X.; et al. 2015. Convolutional neural networks with low-rank regularization. *arXiv preprint arXiv:1511.06067*.
- Vaswani, A.; Shazeer, N.; Parmar, N.; Uszkoreit, J.; Jones, L.; Gomez, A. N.; Kaiser, L.; and Polosukhin, I. 2017. Attention is all you need. *arXiv preprint arXiv:1706.03762*.
- Wang, J.; Cao, B.; Yu, P.; Sun, L.; Bao, W.; and Zhu, X. 2018. Deep learning towards mobile applications. In *2018 IEEE 38th International Conference on Distributed Computing Systems (ICDCS)*, 1385–1393. IEEE.
- Wang, Y.; Tung, H.-Y.; Smola, A.; and Anandkumar, A. 2015. Fast and guaranteed tensor decomposition via sketching. *arXiv preprint arXiv:1506.04448*.
- Williams, A.; Nangia, N.; and Bowman, S. R. 2017. A broad-coverage challenge corpus for sentence understanding through inference. *arXiv preprint arXiv:1704.05426*.

Yang, T.; Andrew, G.; Eichner, H.; Sun, H.; Li, W.; Kong, N.; Ramage, D.; and Beaufays, F. 2018. Applied federated learning: Improving google keyboard query suggestions. *arXiv preprint arXiv:1812.02903*.

Zhang, A. R.; Luo, Y.; Raskutti, G.; and Yuan, M. 2020. ISLET: Fast and optimal low-rank tensor regression via importance sketching. *SIAM journal on mathematics of data science*, 2(2): 444–479.

# Appendix of Paper 10352 Comfetch: Federated Learning of Large Networks on Memory-Constrained Clients via Sketching

## A Sketches

In this section, we review sketching algorithms and data structures which are the most relevant to the implementation of `Comfetch`.

### A.1 Count Sketch

Sketching algorithms seek to compress high-dimensional data structures into lower-dimensional spaces via entry hashing. Sketching was initially proposed by Muthukrishnan et al. (Cormode and Muthukrishnan 2005) as a solution to estimating the frequency of items in a stream (Cormode and Muthukrishnan 2005). Alon et al. (Alon, Matias, and Szegedy 1999) then proposed the eponymous AMS sketch to formalize this setting along with  $\ell_2$ -guarantees of the de-compression of hashed data. The *Count Sketch* is the successor of the AMS sketch, first proposed by Charikar et al. (Charikar, Chen, and Farach-Colton 2002) and outlined in Algorithm 2. The Count Sketch is desired in settings where one is interested in estimating the heavy hitters of a high-dimensional vector, which are the entries with large absolute magnitude relative to other entries.

The Count Sketch data structure contains a collection of  $k$  pairwise-independent hashing maps  $h_i : [d] \rightarrow [c]$  for  $i \in [k]$ , each of which is paired with a sign map  $s_i : [d] \rightarrow \{\pm 1\}$ , for  $i \in [k]$ . Each hash function/sign map pair is used to project a  $d$ -dimensional vector  $x$  into  $c$ -dimensional space, which we refer to as a sketch. Furthermore, we refer to  $c$  as the sketching length and  $k$  as the number of the sketches. Each of the  $k$  sketches is representable as a linear transformation  $H_i x \in \mathbb{R}^c$  for  $i \in [k]$ , where  $H_i \in \mathbb{R}^{c \times d}$  is referred to as a Count Sketch matrix. To “unsketch” or restore a sketch back to  $d$ -dimensional space, we simply multiply by the transpose of  $H_i$ , i.e.,  $\hat{x}_i = H_i^\top H_i x \in \mathbb{R}^d$ , where we use the hat notation to specifically indicate that  $\hat{x}_i$  is merely an approximation of  $x$ . The final approximation  $\hat{x}$  of  $x$  is determined coordinate-wise as  $(\hat{x})_j = \text{median}_{1 \leq i \leq k} \{\hat{x}_i\}_{i=1}^k$  for  $j \in [d]$ .

**Count Sketch matrices** As detailed in the previous section, each sketch has a matrix representation which we now make explicit. Let  $h : [d] \rightarrow [c]$  and  $s : [d] \rightarrow \{\pm 1\}$  be a hash function/sign map pair. The associated Count Sketch matrix  $H$  is representable as the following  $c \times d$  matrix transformation: fixing  $i \in [c]$  and  $j \in [d]$ , we have that  $(H)_{ij} = s(i)$  if  $h(j) = i$  for  $j \in [d]$  and 0 otherwise.

### A.2 Higher-order Sketches

While the Count Sketch is traditionally used to project vectors into lower-dimensional space, it is also possible to sketch higher order tensors. The advantage to sketching higher order tensors is two-fold for us: (1) The  $\ell_2$  guarantees associated with vectorizing a tensor and then using a standard Count Sketch does not scale well with increased modes and does not take advantage of the compact representations

---

Algorithm 2: Count Sketch (Charikar, Chen, and Farach-Colton 2002)

---

**Require:** vector  $x \in \mathbb{R}^d$ , number of hash functions  $k$ , sketch length  $c$

**procedure** INIT( $c, k$ )

- 2: Init sign hashes  $\{s_j\}_{j=1}^k$  and hash functions  $\{h_j\}_{j=1}^k$  ▷ Must be 2-wise independent
- Init  $k \times c$  table of counters  $S$
- 4: **procedure** SKETCH( $i, x_i$ )
- for**  $j = 1, \dots, k$  **do**
- $S[j, h_j(i)] += s_j(i)x_i$
- 6: **procedure** UNSKETCH( $k$ )
- 8: Init length  $k$  array estimates
- for**  $j = 1, \dots, k$  **do**
- estimates[ $k$ ] =  $s_j(i)S[j, h_j(i)]$
- 10: **return**

---

tensors offer. (2) In the forward pass discussion of Section 4, for multi-layer perceptrons, our parameterized weights imitate the count sketch of vectors (namely, the last layer’s output), but for CNN layers, our parametrized weights imitate multiplying matrices by Count Sketch matrices (since the last layer’s output is a matrix), which are not modeled under the usual Count Sketch model. A variety of tensor sketching algorithms exist (Pham and Pagh 2013; Jin, Kolda, and Ward 2019; Wang et al. 2015), but we elect to use the higher-order sketch (HCS) of Shi et al. (Shi and Anandkumar 2019) due to its ease of implementation and resemblance to the Count Sketch.

We leave the details of the HCS algorithm for tensors with order 3 or greater to (Shi and Anandkumar 2019), but for matrices, the method is straightforward. Let  $W \in \mathbb{R}^{d \times d}$ , for simplicity (but one may use rectangular matrices as well). First, in the same manner as the Count Sketch, draw  $k$  pairwise-independent hash functions  $h_i$  and sign maps  $s_i$  of sketching length  $c$ . To sketch  $W$ , simply compute and maintain the collection of products  $\hat{W}_i = H_i^\top H_i W$ . The decomposition (recovery) of  $W$  is denoted  $\hat{W}$ , where coordinate-wise, we have that  $(\hat{W})_{mn} = \text{median}\{\hat{W}_{i_{mn}}\}_{i=1}^k$ , for  $m, n \in [d]$ .

### A.3 Two-Sided Sketching

Our discussion of the HCS in Section A.2 only allows compression along a single mode of a matrix  $W \in \mathbb{R}^{d \times d}$ , but it is possible to sketch along both modes of the matrix, allowing for further compression. In architectural terms, this allows us to decrease the width of each layer and decrease the density of inter-layer connectivity. The procedure is a simple extension of the one-sided HCS. Draw  $k$  pairwise-independent hash functions  $h_i$  and sign maps  $s_i$ . To sketch  $W$ , maintain the collection of products  $\hat{W}_i = (H_{i_1}^\top H_{i_1})W(H_{i_2}^\top H_{i_2})$ , where we note that  $H_{i_1}$  and  $H_{i_2}$  are independently drawn. The decomposition (recovery) of  $W$  is denoted  $\hat{W}$ , where coordinate-wise, we have that  $(\hat{W})_{mn} = \text{median}\{\hat{W}_{i_{mn}}\}_{i=1}^k$ , for  $m, n \in [d]$ .

**Backpropagation Rule** Following the single-sketch model of Section 4, we derive the backpropagation rule for a two-sided sketch. We first require a lemma, which is a basic result of matrix calculus:

**Lemma 2.** Let  $X \in \mathbb{R}^{m \times n}$ ,  $A \in \mathbb{R}^{p \times m}$ ,  $B \in \mathbb{R}^{m \times q}$ , then

$$\frac{\partial AXB}{\partial X} = B \otimes A^\top \quad (10)$$

where  $\otimes$  is the Kronecker product.

We may now use the above result for calculating the gradient of our network after sketching our layers  $\{W_t^\ell\}_{\ell=1}^L$  from both sides, in the same notation as the federated learning setup discussed in Section 2.

**Proposition 3.** Let  $W_t^\ell \in \mathbb{R}^{d \times d}$ ,  $H_1^\ell \in \mathbb{R}^{p \times d}$ ,  $H_2^\ell \in \mathbb{R}^{d \times q}$ . Denote  $\tilde{W}_t^\ell = H_1^\ell W_t^\ell H_2^\ell$ , i.e., a weight matrix sketched from both sides. Then,

$$\nabla_{W_t^\ell} \mathcal{L}(W_t^\ell, z) = (H_2^\ell \otimes H_1^{\ell \top}) \nabla_{\tilde{W}_t^\ell} \mathcal{L} \quad (11)$$

*Proof.* By the chain rule,

$$\frac{\partial \mathcal{L}}{\partial W_t^\ell} = \frac{\partial \mathcal{L}}{\partial \tilde{W}_t^\ell} \frac{\partial \tilde{W}_t^\ell}{\partial W_t^\ell} \quad (12)$$

$$= \frac{\partial \mathcal{L}}{\partial \tilde{W}_t^\ell} (H_1^\ell \otimes H_2^{\ell \top}), \quad (13)$$

where the last line follows by Lemma 2. By transposing both sides of the equation to obtain gradient equations and noting that  $(A \otimes B)^\top = B^\top \otimes A^\top$ , the result follows.  $\square$

## B Proof of Theorem 1

We closely follow the analysis of Karimireddy et al. and Rothschild et al (Karimireddy et al. 2019; Rothschild et al. 2020). To make notation less cumbersome we drop the layer indication and denote our weights as  $W_t \in \mathbb{R}^{d \times d}$ , and denote the sketch recovery of  $W_t$  by  $\hat{W}_t \triangleq RW_t$ , where  $R = H^\top H$  and  $H$  is a Count Sketch matrix of sketching length  $c$  drawn uniformly at random. By Assumption 5 and 6, these recovery transformations are independent of local client data, so our clients are all using the same weights. Our objective is to show  $\min_{t=1,2,\dots,T} \|\nabla_{W_t} f(\hat{W}_t)\| \rightarrow 0$  as  $T \rightarrow \infty$ .

We have then that,

$$\frac{\partial \mathcal{L}(\hat{W}_t, z)}{\partial \hat{W}_t} = \frac{\partial \mathcal{L}(RW_t, z)}{\partial RW_t} \frac{\partial RW_t}{\partial W_t}. \quad (14)$$

So we have the relationship

$$\nabla_{W_t} \mathcal{L}(\hat{W}_t, z) = R^\top \nabla_{RW_t} \mathcal{L}(RW_t, z). \quad (15)$$

We will drop the  $z$  whenever the context is clear. We have then the following useful inequality:

$$\|\nabla_{W_t} f(RW_t)\| = \|R \nabla_{RW_t} f(RW_t)\| \quad (16)$$

$$\leq \|R^\top\| \|\nabla_{RW_t} f(RW_t)\|. \quad (17)$$

Since  $R_i$  only has entries in  $\{-1, 0, 1\}$  with only  $d/c$  non-zero entries per row,  $\|R\|_2 \leq \|R\|_F$ , and  $R$  is  $d \times d$ , we

have that  $\|R_\ell\| \leq d^2/c$ . Hence,  $\|\nabla_{W_t^\ell} f(R_i W_t^\ell, z)\| \leq \frac{d^2}{c} \|\nabla_{R_i W_t^\ell} f(R_i W_t^\ell, z)\|$ , which is a property we will use frequently.

Let  $C(x) = \text{Top-}k(x)$ . We define the temporal sequence  $\tilde{W}_t = W_t - e_t - \frac{\eta\rho}{1-\rho} u_{t-1}$ . This sequence is recursive:

$$\begin{aligned} \tilde{W}_t &= W_{t-1} - C(\eta u_{t-2} + g_{t-1}) + C(\eta(\rho u_{t-2} + g_{t-1}) + e_{t-1}) \\ &\quad - \eta(\rho u_{t-2} + g_{t-1}) - e_{t-1} - \frac{\eta\rho}{1-\rho} z_{t-1} \\ &= W_{t-1} - e_{t-1} - \eta g_{t-1} - \eta\rho u_{t-2} - \frac{\eta\rho}{1-\rho} (\rho u_{t-2} + g_{t-1}) \\ &= W_{t-1} - e_{t-1} - \frac{\eta\rho}{1-\rho} u_{t-2} - \frac{\eta}{1-\rho} g_{t-1} \\ &= \tilde{W}_{t-1} - \frac{\eta}{1-\rho} g_{t-1} \end{aligned}$$

This is almost a stochastic SGD update, but we must prove  $\nabla f(\tilde{W}_t) \approx \nabla f(W_t)$ . To do so, we will provide two results which bound  $\mathbb{E}\|u_t\|^2$  and  $\mathbb{E}\|e_t\|^2$ , respectively.

**Lemma 4.**  $\mathbb{E}\|u_{t-1}\|^2 \leq \left(\frac{d^2 G}{c^2(1-\rho)}\right)^2$ .

*Proof.*

$$\mathbb{E}\|u_t\|^2 = \mathbb{E}\left\|\sum_{i=1}^t \rho^i g_i\right\|^2 \leq \mathbb{E}\left\|\sum_{i=1}^{\infty} \rho^i g_i\right\|^2 \leq \left(\frac{d^2 G}{c(1-\rho)}\right)^2 \quad \square$$

**Proposition 5** ((Karimireddy et al. 2019), Lemma 3).

$$\mathbb{E}\|e_{t-1}\|^2 \leq \frac{4d^4(1-\epsilon^2)\eta^2 G^2}{c^2 \epsilon^2 (1-\rho)^2}.$$

*Proof.*

$$\begin{aligned} \mathbb{E}\|e_{t+1}\|^2 &= \mathbb{E}\|\eta(\rho u_t + g_t) + e_t - C(\eta(\rho u_t + g_t) + e_t)\|^2 \\ &\leq (1-\epsilon) \mathbb{E}\|\eta(\rho u_t + g_t) + e_t\|^2 \\ &\leq (1-\epsilon) \left( (1+\gamma) \|e_t\|^2 + (1+1/\gamma) \eta^2 \|u_t\|^2 \right) \\ &\leq (1-\epsilon) \left( \|e_{t-1}\|^2 + \frac{(1+1/\gamma)d^4 \eta^2 G^2}{c^2(1-\rho)^2} \right) \\ &\leq \sum_{i=0}^{\infty} \frac{((1-\epsilon)(1+\gamma))^i (1+1/\gamma)d^4 \eta^2 G^2}{c^2(1-\rho)^2} \\ &\leq \frac{d^4}{c^2} \frac{(1-\delta)(1+1/\gamma)d^4 \eta^2 G^2}{1 - ((1-\delta)(1+\gamma))} \\ &\leq \frac{4d^4(1-\epsilon)\eta^2 G^2}{c^2 \epsilon^2 (1-\rho)^2}, \end{aligned}$$

where the third inequality, we use Young's inequality; in the fourth inequality, we invoke Lemma 4; and in the last line, we bound everything by choosing  $\gamma = \frac{\epsilon}{2(1-\gamma)}$ .  $\square$

Lastly, we need a result on the quality a multi-sketch recovery (which is equivalent to an HCS) of a matrix, which is provided by Shi et al.:

**Proposition 6** ((Shi and Anandkumar 2019), Theorem B.7). Suppose  $\hat{C}$  is the recovered tensor for  $C = AB$  after applying HCS on  $AB$  with sketching dimension  $c$  along the row mode. We suppose the estimation takes  $d$  independent sketches of  $AB$  and then reports the median of the  $d$  estimates. If  $d = \Omega(\log(1/\delta))$ ,  $c^2 = \Omega\left(\frac{\|C\|_F^2}{\epsilon^2}\right)$ , then with probability at least  $1 - \delta$  there is  $|\hat{C}_{ij} - C_{ij}| \leq \epsilon$ .

*Proof of Theorem 1.* By  $L$ -smoothness of  $f$  we have that

$$\begin{aligned}
\mathbb{E}f(\tilde{W}_{t+1}) &\leq f(\tilde{W}_t) + \left\langle \nabla f(\tilde{W}_t), \mathbb{E}[R(\tilde{W}_{t+1} - \tilde{W}_t)] \right\rangle \\
&+ \frac{L}{2} \mathbb{E} \left\| R(\tilde{W}_{t+1} - \tilde{W}_t) \right\|^2 \\
&\leq f(\tilde{W}_t) + \left\langle \nabla f(\tilde{W}_t), \mathbb{E}[R(\tilde{W}_{t+1} - \tilde{W}_t)] \right\rangle \\
&+ \frac{L}{2} \mathbb{E} \left\| RR^\top \nabla f(RW_t) \right\|^2 \\
&\leq f(\tilde{W}_t) + \left\langle \nabla f(\tilde{W}_t), R\mathbb{E}[g_t] \right\rangle + \frac{\|R\|^4 L}{2} \mathbb{E} \left\| \nabla f(RW_t) \right\|^2 \\
&\leq \mathbb{E}f(\tilde{W}_t) - \frac{\eta}{1-\rho} \langle \nabla f(\tilde{W}_t), Rg_t \rangle + \frac{d^8 L \eta^2 G^2}{2c^4(1-\rho)^2} \\
&= \mathbb{E}f(\tilde{W}_t) - \frac{\eta}{1-\rho} \langle R^\top \nabla f(\tilde{W}_t), R^\top \nabla f(Rw_t) \rangle \\
&+ \frac{Ld^8 \eta^2}{2c^8(1-\rho)^2} G^2 \\
&= \mathbb{E}f(\tilde{W}_t) - \frac{\eta}{1-\rho} \langle R^\top \nabla f(\tilde{W}_t), R^\top \nabla f(R^\ell W_t) \rangle \\
&+ \frac{Ld^8 \eta^2}{2c^8(1-\rho)^2} G^2. \tag{18}
\end{aligned}$$

We will analyze the term  $\langle R^\top \nabla f(\tilde{W}_t), R^\top \nabla f(RW_t) \rangle = R^\top \langle \nabla f(\tilde{W}_t), \nabla f(RW_t) \rangle$ .

$$\begin{aligned}
&R^\top \langle \nabla f(\tilde{W}_t), \nabla f(RW_t) \rangle \\
&= R^\top \langle \nabla f(\tilde{W}_t) - \nabla f(RW_t) + \nabla f(RW_t), \nabla f(RW_t) \rangle \\
&= R^\top \langle \nabla f(RW_t), \nabla f(RW_t) \rangle \\
&+ R^\top \langle \nabla f(\tilde{W}_t) - \nabla f(RW_t), \nabla f(RW_t) \rangle \\
&= \|\nabla_{w_t} f(RW_t)\|^2 + R^\top \langle \nabla f(\tilde{W}_t) - \nabla f(RW_t), \nabla f(RW_t) \rangle
\end{aligned}$$

We analyze the right term in the last inequality. By the mean-value inequality we have that for any  $\gamma > 0$  that,

$$\begin{aligned}
&R_t^\top \langle \nabla f(\tilde{W}_t) - \nabla f(R_t W_t), \nabla f(RW_t) \rangle \\
&\leq \frac{1}{2\gamma} \|\nabla_{w_t} f(R_t W_t)\|^2 + \frac{\gamma d^4}{2c^2} \|\nabla f(\tilde{W}_t) - \nabla f(R_t W_t)\|^2.
\end{aligned}$$

Furthermore,

$$\begin{aligned}
&\frac{\gamma d^4}{2c^4} \|\nabla f(\tilde{W}_t) - \nabla f(R_t W_t)\|^2 \\
&= \frac{\gamma d^4}{2c^4} \|\nabla f(\tilde{W}_t) + \nabla f(W_t) - \nabla f(W_t) - \nabla f(R_t W_t)\|^2 \\
&\leq \frac{\gamma d^4 L^2}{c^4} \|\tilde{W}_t - W_t\|^2 + \frac{\gamma d^4 L^2}{c^4} \|W_t - R_t W_t\|^2 \\
&\leq \frac{\gamma d^4 L^2}{c^4} \|\tilde{W}_t - W_t\|^2 + \frac{\gamma d^4 L^2}{c^4} (1+c) \|W_t\|^2 \\
&\leq \frac{\gamma d^4 L^2}{c^4} \|e_t + \frac{\eta\rho}{1-\rho} u_{t-1}\|^2 + \frac{\gamma d^4 L^2}{c^2} (1+c)^2 B^2 \\
&\leq \frac{4\gamma d^8 L^2 (1-\epsilon) \eta^2 G^2}{c^8 \epsilon^2 (1-\rho)^2} + \frac{\gamma d^4 L^2}{c^4} (1+c)^2 B^2
\end{aligned}$$

where in the first line we used the  $L$ -smoothness of  $f$  and in the last line we invoked Proposition 5 and appealed to the HCS guarantee Proposition 6. Now, without loss of generality we assume that  $\eta < 1$ . Now, there exists a constant  $1 < a < 2$

such that  $\gamma > n^{a+\tau}$ , where  $0 < \tau < 1$  is a tiny constant, and  $\frac{\eta}{2\gamma(1-\rho)} - \frac{\eta}{1-\rho} = \frac{\eta^a}{2(1-\rho)} > 0$ . Plugging these bounds back into equation 18 we have that,

$$\begin{aligned}
&\frac{\eta^a}{2(1-\rho)} \|\nabla_{w_t} f(Rw_t)\|^2 \leq \\
&\mathbb{E}f(\tilde{W}_t) - \mathbb{E}f(\tilde{W}_t) + \frac{\eta}{1-\rho} \frac{4\eta^{a+\tau} d^8 L^2 (1-\epsilon) \eta^2 G^2}{c^8 \epsilon^2 (1-\rho)^2} + \\
&\frac{\eta^{a+\tau} d^4 L^2 (1+c)^2 B^2}{c^4} + \frac{Ld^8 \eta^2 G^2}{2c^8(1-\rho)^2}
\end{aligned}$$

Averaging over  $T$  iterations, we have that

$$\begin{aligned}
\min_{t=1,2,\dots,T} \|\nabla_{w_t} f(RW_t)\|^2 &\leq \frac{1}{T} \sum_{t=1}^T \|\nabla_{w_t} f(RW_t)\|^2 \leq \\
&\frac{2(1-\rho)(f(w_0) - f^*)}{\eta^a T} + \frac{4d^8 L^2 (1-\epsilon) \eta^{3-a} G^2}{c^8 \epsilon^2 (1-\rho)^2} \\
&+ \frac{\eta^\tau d^4 L^2 (1+c)^2 B^2}{c^4} + \frac{L^2 d^8 \eta^{2-a} G^2}{2c^8(1-\rho)}.
\end{aligned}$$

Setting  $\eta = \frac{c^8(1-\rho)}{2d^8 L^2 T^{\frac{3-a}{a}}}$  and noting that  $1 < a < 2$  gives us convergence with a rate of  $\Omega\left(\frac{d^8 L^2 (f(w_0) - f^*)}{c^8 \sqrt{T}} + \frac{4(1-\epsilon)G^2}{T^2 \epsilon^2 (1-\rho)^3} + \frac{c^4(1+c)^2 B^2}{d^4 T} + \frac{G^2}{T}\right)$ .  $\square$

## C Multi-Sketch Comfetch

In this section, we describe how to incorporate the usage of multiple sketches per layer for `Comfetch`, which is described by Algorithm 3.

### C.1 Model Transmission and Download

At iteration  $t$ , the central server first prepares the global model for the transmission by sketching down all the current weights  $\{W_t^\ell\}_{\ell=1}^L$ . We assume that our layers are either convolutional or fully-connected as described in Section 2, and for simplicity, that all our  $W_t^\ell$  are of size  $d \times d$ , but they can be rectangular in practice. For each weight  $W_t^\ell$ , the central server randomly draws Count Sketch matrices  $\{H_i^\ell\}_{i=1}^k$ , where  $H_i^\ell \in \mathbb{R}^{c \times d}$ ,  $c \ll d$  is the sketching length, and transmits  $\{(H_i^{\ell \top}, H_i^\ell W_t^\ell)\}_{i=1}^k$  to a selection of  $N$  uniformly randomly drawn clients, who then download these sketched parameters into local memory. Henceforth, will denote  $\{(\mathcal{U}^\ell, S^\ell(W_t^\ell))\} \triangleq \{(H_i^{\ell \top}, H_i^\ell W_t^\ell)\}_{i=1}^k$  for  $\ell \in [L]$ .

**Cost Complexity** We note that  $k$  corresponds to the number of independent sketches, which is required theoretically to achieve a guarantee on approximating  $W_t^\ell$ , but in practice, we observe in Section 6 that one sketch is sufficient for model convergence. Also note that any  $H_i^\ell$  bijectively corresponds to a hash function  $h_i^\ell: d \rightarrow c$  which is representable as a length  $d$  vector. Hence, in practice, the central server will transmit  $\{(h_i^\ell, H_i^\ell W_t^\ell)\}_{i=1}^k$ , for a total local memory and transmission cost of  $\mathcal{O}((kc+1)d)$ , which in the one-sketch ( $k=1$ ) case is less than the  $O(d^2)$  cost of transmitting the full weight.

### C.2 Client Update

The client  $C_i$  will now conduct a single round of training on the sketched network parameters using their local data. Often in practice, the client distributions  $\mathcal{D}_i$  will be finite and small (Kairouz et al. 2019), so we can assume that the client is always taking the full gradient with respect to the weights, but the algorithm generalizes to stochastic gradients as well.

---

**Algorithm 3: Multi-sketch Comfetch**


---

**Require:** initial weights  $\{W_0^\ell\}_{\ell=1}^L$ , learning rate  $\eta$ , number of iterations  $T$ , momentum parameter  $\rho$ , batch size  $M$  of data, batch size  $N$  of clients  
 Init momentum term  $\{u_0^\ell = 0\}_{\ell=1}^L$   
 2: Init error accumulation term  $e_0 = 0$   
**for**  $t = 1, 2, \dots, T$  **do**  
 4: Init sketching and unsketching procedures  $\{\mathcal{U}^\ell, \mathcal{S}^\ell\}_{\ell=1}^L$   
     Uniformly select at random  $N$  clients  $c_1, c_2, \dots, c_N$   
 6: **loop** {in parallel on clients  $\{c_i\}_{i=1}^N$ }  
     Download parameterized weight pairs  $\{\{\mathcal{U}^\ell, \mathcal{S}^\ell(W_t^\ell)\}_{\ell=1}^L\}$   
 8: **for**  $\ell = 1, 2, \dots, L$  **do**  
     Compute grads  $g_i^\ell = \{\nabla_{H_j W_t} \mathcal{L}(R_i^\ell W_t^\ell, z \sim \mathcal{D}_i)\}_{j=1}^k$  ▷ See equation 26  
 10: Send  $\{g_i^\ell\}_{\ell=1}^L$  to Central Server  
     **end loop**  
 12: **for**  $\ell = 1, 2, \dots, L$  **do**  
     Aggregate restored gradients:  $g_t^\ell = \frac{1}{N} \sum_{i=1}^N \mathcal{G}(g_i^\ell)$  ▷ See equation 27  
 14: Update sketched momentum:  $u_t^\ell = \rho u_{t-1}^\ell + g_t^\ell$   
     Update error feedback:  $e_t = \eta u_t + e_t$   
 16: Approximate gradient with feedback:  $\Delta^t = \text{Top-k}(e_t)$   
     Error accumulation:  $e^{t+1} = e_t - \Delta_t$   
 18: Update weights:  $W_{t+1} = W_t - \Delta_t$   
**return**  $\{W_T^\ell\}_{\ell=1}^L$

---

**Forward pass** Let  $x \in \mathcal{D}_i$  and let  $\{\{\mathcal{U}^\ell, \mathcal{S}^\ell(W_t^\ell)\} \triangleq \{(H_i^{\ell\top}, H_i^\ell W_t^\ell)\}_{i=1}^k\}$  for  $\ell \in [L]$ , where  $L$  is the depth of our network. Following the notations described in Section 2, the forward pass of a fully-connected layer is

$$x^\ell = \sigma(\mathcal{U}^\ell(\mathcal{S}^\ell(W_t^\ell x^{i-1}))), 1 \leq \ell \leq L-1 \quad (19)$$

$$\hat{y} = \mathbf{a}^\top x^L, \quad (20)$$

where  $(\mathcal{U}^\ell(\mathcal{S}^\ell(W_t^\ell))x)_i \triangleq \text{median}_{1 \leq j \leq k} \{(H_j^{\ell\top} H_j^\ell W_t^\ell x)\}$  for any  $x \in \mathbb{R}^d$ , in agreement with the Count Sketch procedure of Algorithm 2. Similarly, for a convolutional ResNet, we have that

$$x^1 = \sqrt{\frac{c_\sigma}{m}} \sigma(\mathcal{U}^1(\mathcal{S}^1(W_t^1))\phi(x^0)) \quad (21)$$

$$x^\ell = x^{\ell-1} + \frac{c_{res}}{L\sqrt{m}} \sigma(\mathcal{U}^\ell(\mathcal{S}^\ell(W_t^\ell))\phi_\ell(x^{\ell-1})), \quad 2 \leq \ell \leq L \quad (22)$$

$$\hat{y} = \langle W_t^L, x^L \rangle, \text{ where } W^L \in \mathbb{R}^{m \times p}. \quad (23)$$

*Remark 1:* We never directly compute a  $d \times d$  weight matrix at any stage.

*Remark 2:* In the convolutional case, where the inputs between layers are matrices,  $H_i W x = H_i (W x)$  can be regarded as a higher-order count sketch (HCS) of  $W x$  as described in Appendix A.

**Backward pass** In order to compute the gradient, we must first clearly define the weights of the modified network. Let  $\{H_i\}_{i=1}^k$  be a random set of  $c \times d$  Count Sketch matrices and let  $x \in \mathbb{R}^d$ .

We have that  $\hat{x}_i := \mathcal{U}(\mathcal{S}(x))_i = \text{median}_{1 \leq j \leq k} \{(H_j^\top H_j x)_i\}$ . If sketch  $H_j$  results in the median recovery of the  $i$ th coordinate of  $x$ , then we have the following representation:

$$\hat{x} = \sum_{i=1}^d E_i H_j^\top H_j x, \quad (24)$$

where  $E_i \in \mathbb{R}^{d \times d}$  is a matrix with 1 at entry  $i, i$  and 0 everywhere else. Therefore, it is possible to define  $\hat{x} = \mathcal{U}(\mathcal{S}(x)) = Ax$  where  $A \in \mathbb{R}^{d \times d}$ . That is, we can represent the Count Sketch recovery of  $x$  as a matrix transformation.

By the above discussion, we can represent  $\mathcal{U}^\ell(\mathcal{S}^\ell(W_t^\ell x^{\ell-1})) = R_i^\ell W_t^\ell x^{\ell-1}$ , where  $R_i^\ell \in \mathbb{R}^{d \times d}$  is referred to as the *recovery matrix*. Hence, the weights of the client network are  $R_i^\ell W_t^\ell$ . Note that we specifically indicate the client index  $i$ , since the recovery matrix will vary depending on the local data.

Now that we have defined the weights of our client models, we may now take gradients. The server will want to receive  $\frac{\partial \mathcal{L}(R_i^\ell W_t^\ell, z)}{\partial W_t^\ell}$  as an approximation of  $\frac{\partial \mathcal{L}(W_t^\ell, z)}{\partial W_t^\ell}$ , but the client will not want to compute  $\frac{\partial \mathcal{L}(R_i^\ell W_t^\ell, z)}{\partial W_t^\ell}$ , since it is of size  $d \times d$ . We will want to transmit a  $\mathcal{O}(kc \times d)$  packet of data which will allow the server to compute  $\frac{\partial \mathcal{L}(R_i^\ell W_t^\ell, z)}{\partial W_t^\ell}$ . To this end, let  $\{H_i^\ell\}_{i=1}^k$  be the set of Count Sketch matrices associated with layer  $\ell$ . Let  $E_{H_i} \in \mathbb{R}^{d \times d}$  denote the matrix which has a 1 at entry  $j, j$  for  $1 \leq j \leq d$  if  $H_i$  contains the median recovery of  $(W_t^\ell x^{\ell-1})_j$  and 0 everywhere else. We have then that,

$$R_i^\ell = \sum_{i=1}^k E_{H_i} H_i W_t^\ell x^{\ell-1}. \quad (25)$$

Therefore, by the chain rule of the total derivative,

$$\frac{\partial \mathcal{L}(R_i^\ell W_t^\ell, z)}{\partial W_t^\ell} = \sum_{i=1}^k \frac{\partial \mathcal{L}(R_i^\ell W_t^\ell, z)}{\partial H_i^\ell W_t^\ell} \frac{\partial H_i^\ell}{\partial W_t^\ell}. \quad (26)$$

Thus, the client will upload  $g_t^\ell \triangleq \{\nabla_{H_i W_t^\ell} \mathcal{L}(R_i^\ell W_t^\ell, z)\}_{i=1}^k$  for all  $\ell \in [L]$ .

*Remark.* We subtly avoided the point that the recovery matrix  $R_i^\ell$  as described is recursively determined by the initial input. Therefore, our sketched weights will not be represented as simple linear transformations of the original weights. However, since the client will clearly be determining gradients through an `autograd`-like library, this will not pose an issue anyways. In our convergence theory, we rectify this issue by assuming that each client trains only on a single data point, which is not far from practical settings, where the local datasets are often small (Kairouz et al. 2019).

**Cost Complexity** If the client chooses to upload the gradients contained within  $g_t^\ell$  in a predefined manner (for example, in the order the sketches were transmitted), then the central server will know which gradients correspond to which sketch, and thus will be able to compute equation without any additional information. Thus, the total communication cost is  $\mathcal{O}(kcd)$ , which in the single-sketch  $k = 1$  scenario, is a strong improvement over the usual uplink cost of  $\mathcal{O}(d^2)$  and even cheaper than the download cost.

*Remark.* The complexity of computing  $R_i^\ell W_t^\ell x^{\ell-1}$  is  $\mathcal{O}(2kcd + k)$ , since the client must individually compute  $H_i^\top H_i W_t^\ell x^{\ell-1}$  for all  $i \in [k]$  to determine the median coordinates. This may not be cheaper than the usual  $\mathcal{O}(d^2)$  matrix-vector multiplication of the original layer, but this is not so relevant to us since computational power of the client is not an important feature of federated learning.

### C.3 Model Update

The Central Server aggregates the  $\{g_i^\ell\}_{i=1}^L$  across all  $i \in [N]$ . We describe the procedure for updating the weight of a fixed layer  $\ell$ . For each  $i \in [N]$ , the server computes

$$\mathcal{G}(g_i^\ell) = \sum_{j=1}^k H_j^{\ell \top} \nabla_{W_j^\ell} \mathcal{L}(R_i^\ell W_t^\ell, z). \quad (27)$$

The server takes an average over the  $\mathcal{G}(g_i^\ell)$  to compute a stochastic gradient of  $f(R^\ell W_t^\ell)$  with respect to  $W_t^\ell$ . That is,

$$\nabla_{W_t^\ell} f(R^\ell W_t^\ell) = \mathbb{E} \frac{1}{N} \sum_{i=1}^N \mathcal{G}(g_i^\ell). \quad (28)$$

The remainder of the model update follows the error-feedback and momentum scheme of `FetchSGD` (Rothchild et al. 2020). Error-feedback allows for the correction of error associated with gradient approximations. In the case of `FetchSGD`, error-feedback corrects the error associated with a taking a sketch and unsketch of the gradients. In the case of `ComFetch`, we are correcting the error associated with using  $\nabla_{W_t^\ell} f(R^\ell W_t^\ell)$  as an approximation of  $\nabla f(W_t^\ell)$ . The reader is encourage to consult the work of Karimireddy et al. and Stich et al. for further details on error-feedback for SGD-like methods (Karimireddy et al. 2019; Stich, Cordonnier, and Jaggi 2018).

*Remark.* We subtly avoided the point that the recovery matrix  $R_i^\ell$  as described is recursively determined by the initial input. Therefore, our sketched weights will not be represented as simple linear transformations of the original weights. However, since the client will clearly be determining gradients through an `autograd`-like library, this will not pose an issue anyways. In our convergence theory, we rectify this issue by assuming that each client trains only on a single data point, which is not far from practical settings, where the local datasets are often small (Kairouz et al. 2019).

If the client chooses to upload the gradients contained within  $g_t^\ell$  in a predefined manner (for example, in the order the sketches were transmitted), then the central server will know which gradients correspond to which sketch, and thus will be able to compute equation 27 without any additional information. Thus, the total communication cost is  $\mathcal{O}(kcd)$ , which in the single-sketch  $k = 1$  scenario, is a strong improvement over the usual uplink cost of  $\mathcal{O}(d^2)$  and even cheaper than the download cost.

*Remark.* The complexity of computing  $R_i^\ell W_t^\ell x^{\ell-1}$  is  $\mathcal{O}(2kcd+k)$ , since the client must individually compute  $H_i^\top H_i W_t x^{\ell-1}$  for all  $i \in [k]$  to determine the median coordinates. This may not be cheaper than the usual  $\mathcal{O}(d^2)$  matrix-vector multiplication of the original layer, but this is not so relevant to us since computational power of the client is not an important feature of federated learning.

### D Additional Language Task Data

In this section, we present additional data in Table 2 and Figure 7 for language tasks not included in the main paper. The results demonstrate that our `ComFetch` preserves accuracy while reducing the size of weights in gates of the LSTM layer by different ratios. We maintain a high test accuracy while reducing the number of parameters from 9607 to 2439. We exclude embedding parameters from the overall parameter counts as they serve as inputs and can be pre-trained.

### E Prediction Error Bound

In this section, we provide a bound on the error between the prediction of a fully-connected multi-layer network and its sketched

Method	Bandwidth Compression	Memory Compression	Number of Params	Test Acc (%)
FedAvg	1	1	9607	47.58
FedAvg-1/2	1	1/2	4423	49.78
FedAvg-1/4	1	1/4	2599	44.01
FedAvg-1/8	1	1/8	1879	25.63
FetchSGD	1	1	9607	86.81
ComFetch	1	1	9607	80.44
ComFetch-1/2	1/2	1/2	5511	81.50
ComFetch-1/4	1/4	1/4	3463	80.57
ComFetch-1/8	1/8	1/8	2439	78.61

**Table 2:** Model accuracies under different memory footprints in clients, for predicting part of speech taggings for MNLI (Williams, Nangia, and Bowman 2017) sentences using `LSTM`. We exclude embeddings from parameter counts as they serve as inputs and can be pretrained.

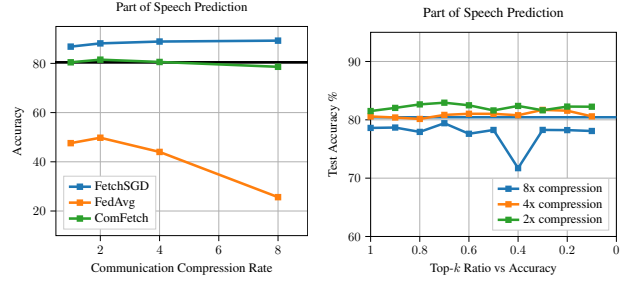


**Figure 7:** Test accuracy achieved on predicting part of speech taggings for MNLI (Williams, Nangia, and Bowman 2017) sentences. On the left, we present quantitative comparisons to other methods. The horizontal line reflects the simple baseline where no compression is applied during training. On the right, we report the test accuracy with different compression rate while varying the  $K$  ratio. `FetchSGD` only compresses the network weights during communication, but each client still needs to decompress the entire network locally to perform training.

counterpart. We denote by  $\phi : \mathbb{R}^d \rightarrow \mathbb{R}^d$ , the ReLU (rectified linear unit), where for any  $x \in \mathbb{R}^d$ , we have that  $(\phi(x))_i = \max((x)_i, 0)$ . For ease (and an abuse) of notation, we let  $\psi \circ W_L \circ \psi \circ W_{L-1} \circ \dots \circ \psi \circ W_1 x = \phi(W_L(\phi(W_{L-1}(\dots(\phi(W_1 x))))))$ , where  $W_\ell \in \mathbb{R}^{d \times d}$  for  $1 \leq \ell \leq L$ ,  $x \in \mathbb{R}^d$ , and we are freely allowing  $W_1$  to act as both a linear transformation and a matrix multiplication (i.e.,  $W_1 \circ x = W_1 x$ ).

**Theorem 7.** *Let*

$$\hat{y}_L = \psi \circ W_L \circ \psi \circ W_{L-1} \circ \dots \circ \psi \circ W_1 \circ x, \quad (29)$$

$W_\ell \in \mathbb{R}^{d \times d}$  for  $1 \leq \ell \leq L$ ,  $x \in \mathbb{R}^d$ , and  $\psi$  is the ReLU activation function. Now let

$$\tilde{y}_L = \psi \circ H_L^{-1} H_L W_L \circ \psi \circ H_{L-1}^{-1} H_{L-1} W_{L-1} \circ \dots \circ \psi \circ H_1^{-1} H_1 W_1 x, \quad (30)$$

$$\dots \circ \psi \circ H_1^{-1} H_1 W_1 x, \quad (31)$$

where  $H_\ell^{-1} H_\ell W_\ell$  reflects a count sketch recovery of  $W_\ell$ . If for each  $H_\ell^{-1} H_\ell W_\ell$  we have chosen each sketching length of  $W_\ell$  as  $c = \Omega(\|W_\ell\|_F^2 / \epsilon^2)$  and the number of independent sketches as  $\mathcal{O}(\log \frac{d}{\delta})$ , for  $0 < \delta < 1$ , then with  $(1 - \delta)^L$  probability we have that

$$\|\tilde{y}_L - \hat{y}_L\| \leq \sum_{j=1}^L g_j(x), \quad (32)$$

where  $g_j(x) = \lambda_j \lambda_{j+1} \dots \lambda_L \|x\| d^2 \epsilon^2 \prod_{n=1}^{j-1} \hat{\lambda}_n$ ,  $\lambda_i$  is the maximum singular value of  $W_i$ , and  $\hat{\lambda}_i$  is the maximum singular value of  $H_\ell^{-1} H_\ell$ . We let  $g_0 = d^2 \epsilon^2 \|x\|$ .

*Proof.* We proceed by induction on the number of layers  $L$ . For simplicity, we denote  $\hat{W}_i := H_i^{-1} \circ H_i \circ W_i$ . For  $L = 1$ , we have that

$$\|\psi \circ \hat{W}_i x - \psi W_i x\| \leq \|\hat{W}_i - W_i\| \|x\| \leq d^2 \epsilon^2 \|x\| = g_0, \quad (33)$$

where the first inequality follows by the fact the ReLU  $\psi$  is 1-Lipschitz and the second inequality follows by HCS guarantee Lemma 6 our the prescribed width and depth of our sketches,  $\mathcal{O}(\frac{1}{\epsilon^2} \log \frac{d}{\delta})$ . Assume the hypothesis holds for  $L = k$  layers, then for  $L = k + 1$  layers we have that

$$\|\tilde{y}_{k+1} - \hat{y}_{k+1}\| = \|\psi \circ \hat{W}_{k+1} \circ \tilde{y}_k - \psi \circ W_{k+1} \circ \hat{y}_k\| \quad (34)$$

$$\leq \|\hat{W}_{k+1} \circ \tilde{y}_k - W_{k+1} \circ \hat{y}_k\| \quad (35)$$

$$\leq \|\hat{W}_{k+1} \circ \tilde{y}_k - W_{k+1} \circ \tilde{y}_k + W_{k+1} \circ \tilde{y}_k - W_{k+1} \circ \hat{y}_k\| \quad (36)$$

$$\leq \|\hat{W}_{k+1} \circ \tilde{y}_k - W_{k+1} \circ \tilde{y}_k\| + \|W_{k+1} \circ \tilde{y}_k - W_{k+1} \circ \hat{y}_k\| \quad (37)$$

$$\leq \|\hat{W}_{k+1} - W_{k+1}\| \|\tilde{y}_k\| + \|W_{k+1}\| \|\tilde{y}_k - \hat{y}_k\| \quad (38)$$

$$\leq d\epsilon^2 \|x\| \prod_{n=1}^k \hat{\lambda}_n + \lambda_{k+1} \sum_{j=1}^k g_j \quad (39)$$

$$= \sum_{j=1}^{k+1} g_j, \quad (40)$$

where the second to last inequality follows by applying the inductive hypothesis to the right term  $\|\tilde{y}_k - \hat{y}_k\|$  and noting that for the left term,

$$\|\tilde{y}_k\| = \|\psi \circ \hat{W}_k \circ \psi \hat{W}_{k-1} \circ \dots \circ \hat{W}_1 x\| \quad (41)$$

$$\leq \|x\| \prod_{i=1}^k \|\hat{W}_i\| \leq \hat{\lambda}_i \|x\|. \quad (42)$$

The probabilistic guarantee of  $(1 - \delta)^L$  follows by the independence of each individual layer sketching.  $\square$

The above result theoretically demonstrates that the noise is controllable via increased sketched length and number of independent sketches, and in general, requires increased space complexity as  $L$  increases.